VIBRATION ANALYSIS FOR PIEZOCERAMIC CIRCULAR PLATES WITH V-NOTCHES. PART 1: THEORY

C.-H. Huang * **Y.-Y. Chen**

Department of Mechanical Engineering
Chien Hsin University of Science and Technology
Taoyuan County, Taiwan

ABSTRACT

In this paper the transverse vibration characteristics of piezoceramic circular plates with V-notches are investigated theoretically through use of the Ritz's method incorporated with the defined equivalent constants. The Ritz's method is employed with two sets of admissible displacement functions, algebraic-trigonometric polynomials and corner functions, to guarantee convergence sufficiently and represent the stress singularity, respectively. Moreover, the equivalent constants derived by comparing the characteristic equations of transverse vibration between isotropic and piezoceramic disks are applied to suspend the electrical field consideration regarding the piezoelectricity. With the aid of theoretical analysis, the non-dimensional frequency parameters of transverse vibration modes for completely free V-notching circular plates are exhibited; in addition, the frequency variations depending on various notch angles and depths are explored. Numerical calculations using the finite element method (FEM) are performed and the results are compared with the theoretical analysis. It is shown that the resonant frequencies predicted by theoretical analysis and calculated by FEM are in good agreement.

Keywords: Vibration, Piezoceramic plate, Equivalent constants.

1. INTRODUCTION

Piezoelectricity describes the phenomenon in which the material generates electric charge when subjected to stress and, conversely, generates strain when the electric field is applied. Owing to the simple configuration and high performance, the piezoelectric materials have been widely used in electromechanical sensors, actuators, non-destructive testing devices as well as electro-optic modulator. Especially for the piezoelectric ceramics made of lead zirconate titanate (PZT), numerous investigations have been performed on the disk or annulus types in the analysis and applications, *e.g.* Langevin transducers and ultrasonic motors. The vibration characteristics of piezoelectric materials are determined by three-dimensional equations of the linear elasticity, the Maxwell equation, and piezoelectric constitutive equations (Tiersten [1]); nevertheless, it is difficult to obtain complete solutions for even a simple geometry. On account of the complication as mentioned above, there are two numerical methods that are usually used to study the vibration problem of piezoelectric materials; one is the variational approximation method and the other is finite element analysis. Holland [2] used the Rayleigh-Ritz method to study the extensional modes of rectangular piezoelectric plates and classified them into four distinct symmetry types. Eer Nisse [3] applied the calculus of variation to the analysis of piezoelectric disks, and compared the results with the experimental results obtained by Shaw [4]. Kunkel *et al.* [5] studied the vibration modes of PZT-5H ceramics disks concerning the diameter-to-thickness (D/T) ratio ranging from 0.2 to 10. Due to the great flexibility and extensive applicability, the finite element method has become the alternative method to the analysis of piezoelectric material in various configurations. Guo *et al.* [6] presented the results for PZT-5A piezoelectric disks with D/T of 20 and 10. In that study there were five types of modes classified according to the mode shape characteristics, and the physical interpretation was clarified. Ivina [7] studied the symmetric modes of vibration for circular piezoelectric plates to determine the resonant and anti-resonant frequencies, radial mode configurations, and the optimum geometrical dimensions to maximize the dynamic electromechanical coupling coefficient. The finite element method is a powerful tool, but sometimes an analytical solution is needed to get a deep and clear understanding of the characteristics of resonant vibrations for piezoceramic plates.

The characteristics of piezoceramic plates, which have crystal symmetry class C_{6mm}, can indeed serve as the transverse isotropic plate for vibration investigation. This reveals that the characteristic equation of transverse vibration for the piezoceramic plate can be obtained through its use for the isotropic plate. The characteristic equation of transverse vibration can be derived in terms of defined material constants, the

* Corresponding author (chhuang@uch.edu.tw)

DOI : 10.1017/jmech.2014.53
Copyright © 2014 The Society of Theoretical and Applied Mechanics, R.O.C.
https://doi.org/10.1017/jmech.2014.53 Published online by Cambridge University Press

equivalent Poisson's ratio $\bar{\nu}$ and bending stiffness $\bar{D}$. By using the proposed method, namely, the equivalent constant method [8], the electrical field consideration is suppressed and only the characteristic equations of isotropic plates, which are available in the literature, are needed. Huang and Chen [9] used the equivalent constant methodology to explore the vibration characteristics of piezoceramic rectangular plates with clamped-free-free-free and clamped-free-clamped-free boundary conditions, which results were verified by numerical and experimental investigations.

The equivalent constant methodology was successfully applied to the vibration analysis for complete piezocramic rectangular plates in [9]; nevertheless, the minority of literature addressed about piezoceramic plates had been carried out on the plates with faults, for instance, notches or cracks. In light of the motivation, the transverse vibration analysis of piezoceramic circular plates with V-notches is investigated in this work. Prior to manipulating the vibration analysis of piezoceramic circular plates with V-notches, as mentioned above, it is necessary to comprehend the similar problem for V-notching isotropic plates. Leissa *et al.* [10] employed the novel Ritz's method, which incorporated a complete set of algebra-trigonometric polynomials in conjunction with an admissible set of corner functions, to study the vibrations of isotropic circular plates with V-notches or radial cracks. This approach was also successfully applied to investigate free vibration for circular plates with V-notches of various edge conditions [11,12]. In this paper, we utilize the method proposed by Leissa *et al.* [10] along with the equivalent constants to perform the theoretical vibration analysis for piezoceramic circular plates with V-notches. By varying the corner angles and depths of the notch, the sectorial plate and the plate with a sharp notch are included in the study. To validate the theoretical calculations, numerical computations based on a finite element package are also presented, and good agreements are found in comparison with the theoretical analysis. Based on the theoretical analysis, the dimensionless frequency parameter is introduced to discuss the resonant frequency variation with respect to the effect of corner angles and depths of the notches.

2. METHODOLOGY: THE RITZ'S METHOD AND EQUIVALENT CONSTANTS

Figure 1 shows the geometric configuration of a completely free circular plate having a V-notch, in which the origin of polar coordinates coincides with the vertex of the notch. The transverse displacement w with angular frequency ω is given by

$$w = w(r, \theta, t) = W(r, \theta)\sin \omega t\,, \tag{1}$$

where t is the time.

The maximum strain energy $V_{\max}$ and kinetic energy $T_{\max}$ for the plate during the vibration cycle is expressed as,

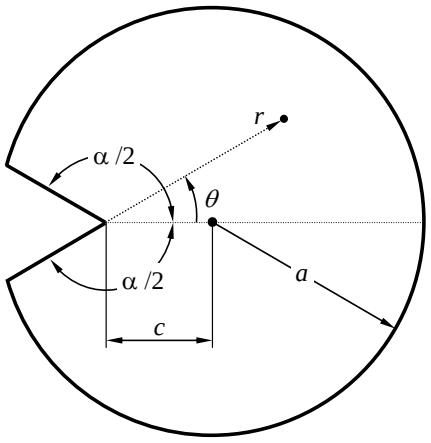


Fig. 1 Geometry and coordinate system of the circular plate with a V-notch.

$$V_{\max} = \frac{D}{2}\iint_A \left[(\kappa_r + \kappa_\theta)^2 - 2(1-\nu)(\kappa_r\,\kappa_\theta - \kappa_{r\theta}^2)\right] dA\,, \tag{2}$$

and

$$T_{\max} = \frac{1}{2}\rho\omega^2 \iint_A W^2 dA\,, \tag{3}$$

respectively, where $D = Eh^3 / 12(1 - \nu^2)$ is the bending stiffness, E is Young's modulus, h is plate thickness, ν is Poisson's ratio, and ρ is material density. The symbols κ_r, κ_θ, and $\kappa_{r\theta}$, in Eqs. (2) and (3), are, respectively, maximum bending curvatures in r and θ directions and twisting curvature which are defined as

$$\kappa_r = \frac{\partial^2 W}{\partial r^2}\,,\quad \kappa_\theta = \frac{1}{r}\frac{\partial W}{\partial r} + \frac{1}{r^2}\frac{\partial^2 W}{\partial \theta^2}\,,\quad \kappa_{r\theta} = \frac{\partial}{\partial r}\left(\frac{1}{r}\frac{\partial\, W}{\partial \theta}\right). \tag{4}$$

The displacement trial functions are expressed as the combination of two sets of admissible functions [10]

$$W = W_p + W_c\,, \tag{5}$$

where W_p is the algebraic-trigonometric polynomials and W_c the corner function. The W_p can be written as

$$W_{p,S} = \sum_{m=0,2,4}^{M_1}\sum_{n=0,2,4}^{m} A_{mn}\, r^m \cos n\theta + \sum_{m=1,3,5}^{M_2}\sum_{n=1,3,5}^{m} A_{mn}\, r^m \cos n\theta\,, \tag{6.1}$$

for the symmetric vibration modes and

$$W_{p,A} = \sum_{m=2,4}^{M_3}\sum_{n=2,4}^{m} B_{mn}\, r^m \sin n\theta + \sum_{m=1,3,5}^{M_4}\sum_{n=1,3,5}^{m} B_{mn}\, r^m \sin n\theta\,, \tag{6.2}$$

for the anti-symmetric vibration modes.

When the sufficient terms of the series are employed to perform the numerical calculations, the exact resonant frequencies can be obtained theoretically. As the stress singularity, however, is present at the vertex of the V-notch, the calculation procedure is quite tedious. In order to accelerate convergence and simulate the

https://doi.org/10.1017/jmech.2014.53 Published online by Cambridge University Press

corner singularity, the corner function W_c is introduced and expressed as [10]

$$W_c = \sum_{k=1}^{K} C_k W_{ck}^* , \tag{7}$$

where C_k are arbitrary coefficients and W_{ck}^* is expressed as [13]

$$W_{ck}^* = r^{\lambda_k+1}\left[a_k \sin(\lambda_k+1)\,\theta + b_k \cos(\lambda_k+1)\theta + c_k \sin(\lambda_k-1)\,\theta + d_k \cos(\lambda_k-1)\,\theta\right]. \tag{8}$$

For the free boundary condition along the edges of the notch ($\theta = \pm\alpha/2$), the circumferential bending moment

$$M_\theta = -D(\kappa_\theta + \nu\kappa_r), \tag{9.1}$$

and the Kelvin-Kirchhoff edge reaction

$$V_\theta = -D\left[\frac{1}{r}\frac{\partial}{\partial\theta}(\kappa_r + \kappa_\theta) + (1-\nu)\frac{\partial\kappa_{r\theta}}{\partial r}\right], \tag{9.2}$$

must be equal to zero. By substituting Eq. (8) into Eqs. (4), (9.1), and (9.2), the characteristic equation of eigenvalues λ_k is found and classified into two types:

(1) For symmetric modes

characteristic equation: $\sin(\lambda_k\alpha) = \dfrac{1-\nu}{3+\nu}\lambda_k \sin\alpha$.

corner function:

$$W_{ck,S}^* = r^{\lambda_k+1}\left\{\frac{(1-\nu)\lambda_k + (3+\nu)}{(\lambda_k+1)(\nu-1)}\frac{\sin\left[(\lambda_k-1)\alpha/2\right]}{\sin\left[(\lambda_k+1)\alpha/2\right]}\cos(\lambda_k+1)\,\theta + \cos(\lambda_k-1)\,\theta\right\}. \tag{10}$$

(2) For anti-symmetric modes

characteristic equation: $\sin(\lambda_k\alpha) = -\dfrac{1-\nu}{3+\nu}\lambda_k \sin\alpha$.

corner function:

$$W_{ck,A}^* = r^{\lambda_k+1}\left\{\frac{(1-\nu)\lambda_k + (3+\nu)}{(\lambda_k+1)(\nu-1)}\frac{\cos\left[(\lambda_k-1)\alpha/2\right]}{\cos\left[(\lambda_k+1)\alpha/2\right]}\sin(\lambda_k+1)\,\theta + \sin(\lambda_k-1)\,\theta\right\}. \tag{11}$$

By substituting Eqs. (6), (7), (8), (10), and (11) into Eqs. (2) ~ (4) and employing the following equations

$$\frac{\partial}{\partial A_{mn}}(V_{\max} - T_{\max}) = 0, \quad \frac{\partial}{\partial B_{mn}}(V_{\max} - T_{\max}) = 0, \quad \frac{\partial}{\partial C_k}(V_{\max} - T_{\max}) = 0, \tag{12}$$

there results a set of homogeneous algebraic equations regarding the constants A_{mn}, B_{mn}, and C_k. The eigenvalues, which represent the resonant frequencies, can be obtained by vanishing the determinant of the coefficient matrix.

As seen in Eqs. (2) and (4), the transverse resonant frequencies of the vibrating thin plate vary with the material constants, bending stiffness D and Poisson's ratio ν. For the piezoceramic plate with crystal symmetry class C_{6mm}, the characteristics of transverse vibration can serve as those for the isotropic plate. It reveals that the resonant frequencies of transverse vibration for the piezoceramic plate can be obtained by the manipulation of isotropic plates. To perform the corresponding methodology, the equivalent Poisson's ratio $\bar{\nu}$ and bending stiffness $\bar{D}$ are introduced and defined in [8] as

$$\bar{\nu} = \frac{2-(1-\nu_p)(2-k_p^2)}{2-(1-\nu_p)k_p^2}, \tag{13}$$

$$\bar{D} = \frac{h^3}{12}\cdot\frac{2-(1-\nu_p)k_p^2}{2s_{11}^E(1-\nu_p^2)(1-k_p^2)}, \tag{14}$$

in which $\nu_p = -\dfrac{s_{12}^E}{s_{11}^E}$ is the planar Poisson's ratio, $k_p = \sqrt{\dfrac{2d_{31}^2}{\varepsilon_{33}^T s_{11}^E(1-\nu_p)}}$ is the planar electromechanical coupling coefficient, s_{11}^E and s_{12}^E are the compliance constants at constant electrical field, d_{31} is the piezoelectric constant, and $\varepsilon_{11}^T, \varepsilon_{33}^T$ is the dielectric constant at constant stress. By replacing ν and D in Eq. (2) by $\bar{\nu}$ and $\bar{D}$ respectively, the eigenvalues of resonant frequencies can be derived for the piezoceramic circular plates with V-notches.

3. THEORETICAL AND NUMERICAL RESULTS

The completely free piezoceramic circular plate having a V-notch as shown in Fig. 1 with the radius a = 20 mm and thickness h = 0.5 mm is selected to perform theoretical investigations, the material properties and modal number of which are listed in Table 1. The polarization is in the thickness direction, and two opposite surfaces of the plate are completely coated with electrodes. There are two independent variables are employed in the geometric configuration: "c" is the distance between notch tip and center of the plate, and "α" is the corner angle. As referring to Fig. 1, the $1 - (c/a)$ is termed as relative depth of the notch, and $(360° - \alpha)$ the notch angle.

Table 2 shows the theoretical and numerical results of the first six resonant frequencies for V-notching circular plates with different corner angles (α) and notch depth ratios (c/a). The notch depth ratio c/a ranges from 0 to 0.75 in 0.25 interval in each step. The corner

https://doi.org/10.1017/jmech.2014.53 Published online by Cambridge University Press

Table 1 Material properties of the piezoceramics PIC-151 (Physik Instrument Company).

Piezoelectric constants	
s_{11}^E (10^{-12} m^2/N)	16.83
s_{33}^E	19.0
s_{12}^E	−5.656
s_{13}^E	−7.107
s_{44}^E	50.96
$c_{66}^E = (c_{11}^E - c_{12}^E)/2$	44.97
d_{31} (10^{-10} m/V)	−2.14
d_{33}	4.23
d_{15}	6.1
ε_{11}^T (10^{-9} F/m)	17.134
ε_{33}^T	18.665
ρ (kg/m^3)	7800

Table 2 Results of the resonant frequencies obtained by theory for the completely free piezoceramic circular plates with V-notches. Square brackets represent the values calculated by FEM.

α	c/a	Mode number					
		1 (Hz)	2 (Hz)	3 (Hz)	4 (Hz)	5 (Hz)	6 (Hz)
180°	0	1247.2 [1247.4]	1599.5 [1597.1]	3190.6 [3199.4]	3273.5 [3274.5]	5247.5 [5259.8]	5810.3 [5811.7]
	0.25	1140.8 [1142.5]	1233.8 [1235.0]	2470.9 [2485.7]	2935.6 [2948.1]	4095.0 [4114.4]	4195.2 [4241.8]
	0.5	1028.3 [1032.7]	1076.8 [1081.3]	2089.9 [2108.0]	2583.6 [2616.9]	3084.0 [3113.2]	3926.5 [3972.7]
	0.75	925.50 [935.20]	997.73 [1008.4]	1981.3 [1999.8]	2255.9 [2320.8]	2477.2 [2530.9]	3899.0 [4061.2]
270°	0	776.01 [775.43]	1067.2 [1068.2]	1703.3 [1713.2]	2195.4 [2214.3]	3262.9 [3267.9	3316.5 [3379.3]
	0.25	793.46 [788.02]	1028.4 [1027.1]	1725.9 [1730.1]	2024.5 [2029.1]	2861.4 [2890.3]	3647.3 [3682.8]
	0.5	841.66 [844.01]	976.38 [977.89]	1853.5 [1864.0]	1978.5 [1997.0]	2479.6 [2511.6]	3622.1 [3735.3]
	0.75	890.27 [906.33]	928.85 [952.39]	1969.0 [1979.5]	2080.9 [2174.3]	2222.4 [2341.4]	3676.1 [3993.5]
359°	0	474.91 [474.41]	739.58 [728.95]	1306.2 [1326.0]	1528.3 [1496.5]	2047.9 [2078.9]	2562.3 [2637.3]
	0.25	646.04 [646.70]	806.21 [802.19]	1412.8 [1434.8]	1708.7 [1681.1]	2053.5 [2094.8]	2690.0 [2797.5]
	0.5	814.53 [823.50]	859.98 [865.04]	1726.5 [1760.7]	1888.0 [1878.1]	2049.8 [2107.0]	2932.8 [3068.4]
	0.75	891.82 [912.91]	895.44 [914.23]	1973.4 [1978.0]	2077.2 [2191.4]	2103.4 [2208.1]	3623.2 [3966.5]
Cracked plate	0	[472.41]	[725.41]	[1319.1]	[1495.1]	[2070.3]	[2625.8]
	0.25	[645.76]	[799.76]	[1429.3]	[1680.2]	[2088.7]	[2786.7]
	0.5	[823.51]	[863.79]	[1758.5]	[1878.0]	[2102.9]	[3060.7]
	0.75	[912.98]	[913.90]	[1977.9]	[2191.7]	[2207.0]	[3966.9]
Circular plate		906.65 [920.72]	1979.9 [1978.2]	2148.2 [2225.2]	3825.7 [4072.0]	4319.7 [4311.5]	5933.4 [6544.2]

angle α is taken to be 180°, 270°, and 359°; that is, only the re-entrant angles are considered to create the V-notching plate as shown in Fig. 1. The "cracked plate" in Table 2 represents the piezoceramic circular plate with a radial sharp crack emanating from the edge. The FEM calculations of resonant frequencies are carried out by the ABAQUS finite element package [14]. The 20-node three-dimensional solid piezoelectric element "C3D20RE", standing for the 20-node quadratic brick element with reduced integration in ABAQUS, is selected for the numerical analysis. The electrical potential on the surfaces of piezoceramic plates is specified as "zero" for the closed-circuit condition simulation and the resonant frequency extraction. Herein the theoretical derivation concentrates the attention on resonant frequency extraction to compare with the FEM calculation. Consequently, the damping effects are neglected in the theoretical and numerical results. Owing to stress concentration at the notch tip, it is necessary to manipulate the element mesh in the vicinity of the notch tip. By placing the first node away from that point at one quarter of the distance to the second point, named "quarter point" method, the stress near the notch tip will behave as a square root singularity. The results presented in Table 2 show good agreements between the theoretical prediction and numerical calculation. To obtain the well-conditioned convergence and decrease the numerical computation time, as referring to [10], five corner functions associated with 30 polynomial terms are employed in this study. The error between theoretical and numerical results can be approved somewhat by increasing the number of algebraic-trigonometric polynomials and corner functions. However, the thickness of the V-notching circular plate shows significant influence on the theoretical and numerical results. This is because the two-dimensional plate hypotheses and three-dimensional element simulations are employed for theoretical and FEM calculations, respectively.

Figure 2 demonstrates the numerical results for the first six mode shapes of the V-notching piezoceramic sectorial plates ($c/a = 0$) with α = 180°, 270°, and 359°. In this figure, we indicate the phase of displacement for numerical results as dark or light lines, with the dark lines in opposite direction to the light lines. The transition from dark lines to light ones corresponds to zero displacement lines, or called nodal lines. Because the existence of a V-notch will destroy the axisymmetric characteristics and introduce new free boundaries of the circular plate, the nodal lines of the V-notching circular plate are no longer simply composed of diameters and circles as in the case of a complete circular plate.

In order to discuss the influence of the corner angle and notch depth ratio on the resonant frequency, the resonant frequency f is expressed in terms of a non-dimensional frequency parameter $\bar{\lambda}$ as

$$\bar{\lambda} = 2\pi f a^2 \sqrt{\frac{\rho h}{\bar{D}}}.$$

Figures 3 ~ 6 show the dependence of frequency parameter $\bar{\lambda}$ on corner angles α ranging from 180° to

https://doi.org/10.1017/jmech.2014.53 Published online by Cambridge University Press

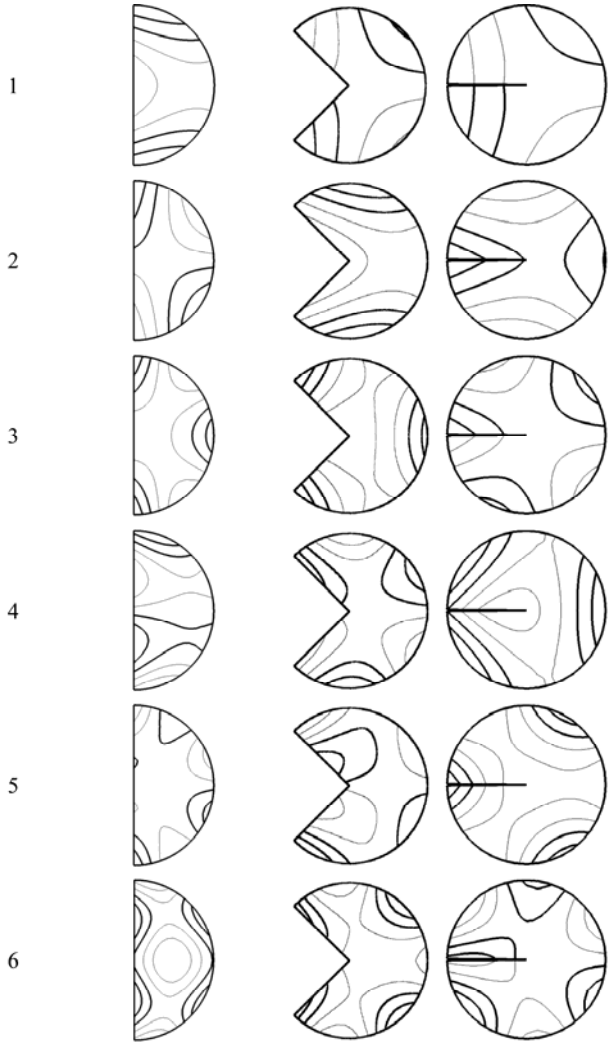


Fig. 2 The transverse vibration mode shapes for the V-notching piezoceramic plate ($c/a = 0$).

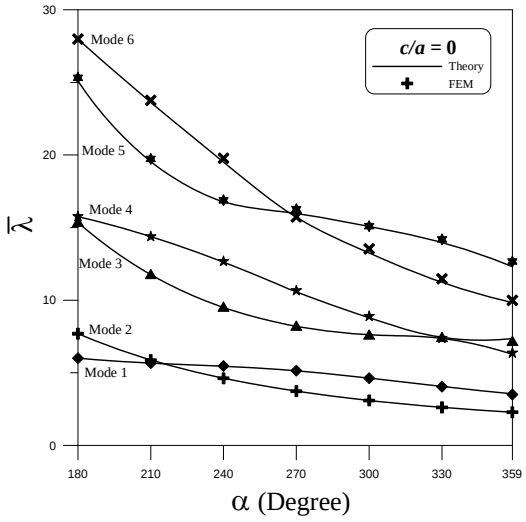


Fig. 3 The dependence of frequency parameter ($\bar{\lambda}$) versus corner angle (α) for the V-notching piezoceramic plate with $c/a = 0$.

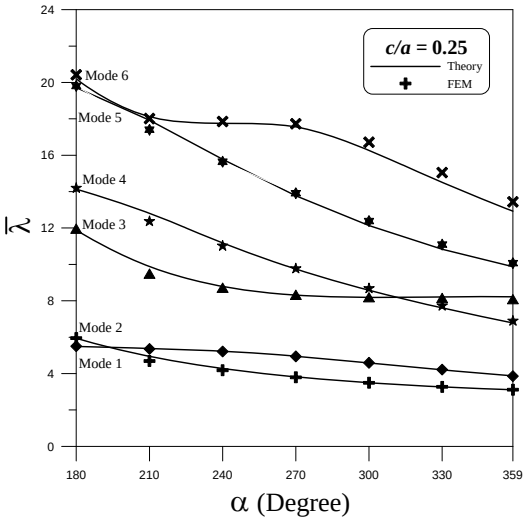


Fig. 4 The dependence of frequency parameter ($\bar{\lambda}$) versus corner angle (α) for the V-notching piezoceramic plate with $c/a = 0.25$.

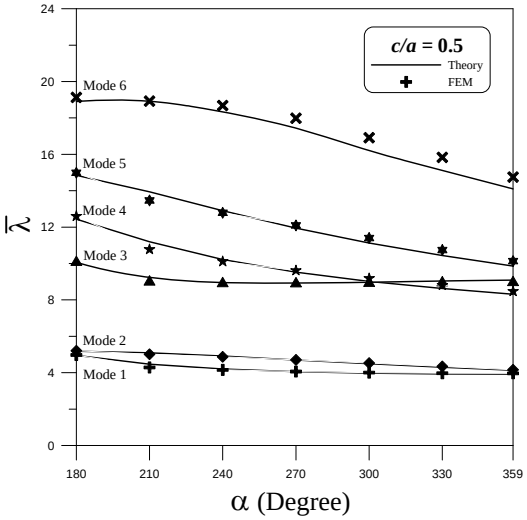


Fig. 5 The dependence of frequency parameter ($\bar{\lambda}$) versus corner angle (α) for the V-notching piezoceramic plate with $c/a = 0.5$.

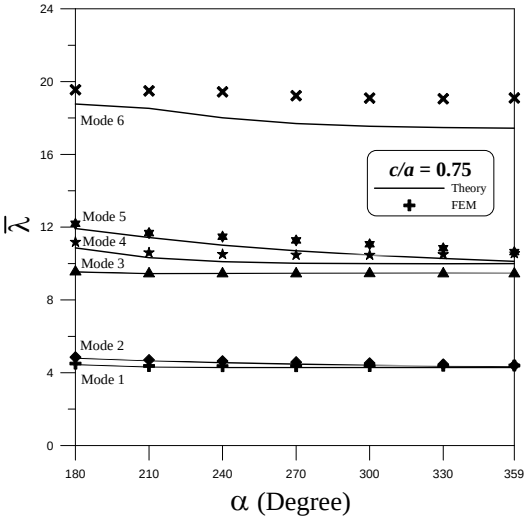


Fig. 6 The dependence of frequency parameter ($\bar{\lambda}$) versus corner angle (α) for the V-notching piezoceramic plate with $c/a = 0.75$.

https://doi.org/10.1017/jmech.2014.53 Published online by Cambridge University Press

359° for the first six vibration modes, in which $\bar{\lambda}$ is plotted against corner angle α to exhibit properly the resonant frequency variation. As expected from the fact that the stiffness of the V-notching circular plate decreases as the corner angle increases, the resonant frequencies decrease with increasing corner angle. Besides, when the corner angle increases, the mass of the V-notching circular plate increases and the resonant frequencies vary inversely proportional to the corner angle. Through use of finite element calculation to trace the mode shape variation, it is found that in Fig. 3, the order of modes 1 and 2 exchange as the corner angle $\alpha \geq 210°$. This phenomenon also occurs for modes 3 and 4 as $\alpha \geq 330°$ and so do the modes 5 and 6 as $\alpha \geq 270°$. The similarities are also presented in Figs. 4 ~ 6. Hence, the order of mode shapes is not permanent and may change in light of different values of α. Whenever the curves of frequency parameter intersect at certain α value, the transition of vibration modes occurs and the order of these two modes exchanges with each other.

For the specified corner angles α = 180° and 359°, the variation in the non-dimensional frequency parameter ($\bar{\lambda}$) for different notch depth ratios (c/a) is shown in Figs. 7 and 8. It is indicated that c/a = 0 stands for the sectorial plate and c/a = 1 for the complete circular plate. As can be seen in Figs. 7 and 8, the first six vibration modes for V-notching circular plates degenerate to the first four modes for complete circular plates. The first and second modes of V-notching circular plates with free boundary conditions obviously degenerate to the first mode of complete circular plates for which vibration mode shape comprises two orthogonal nodal diameters. In Fig. 7, the resonant frequencies decrease gradually for increased c/a values owing to increasing the mass of V-notching circular plates. However, the frequency variation tendency shown in Fig. 8 is obviously different from that shown in Fig. 7. This phenomenon implies that the rigidity of the V-notching circular plate decreases as the depth of notch increases, *i.e.*, as the c/a value decreases.

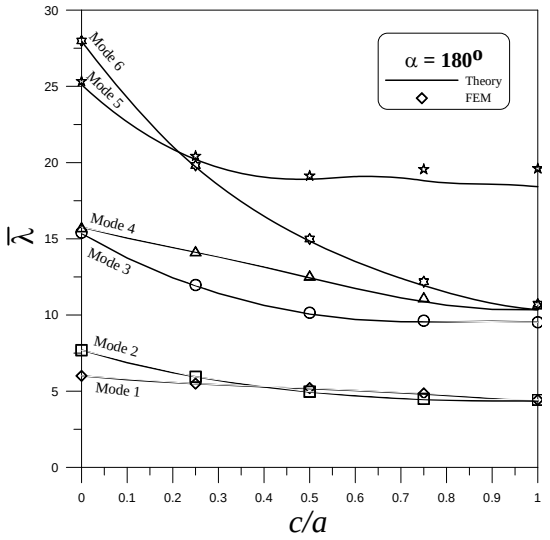


Fig. 7 The dependence of frequency parameter ($\bar{\lambda}$) versus notch depth ratios (c/a) for the V-notching piezoceramic plate with α = 180°.

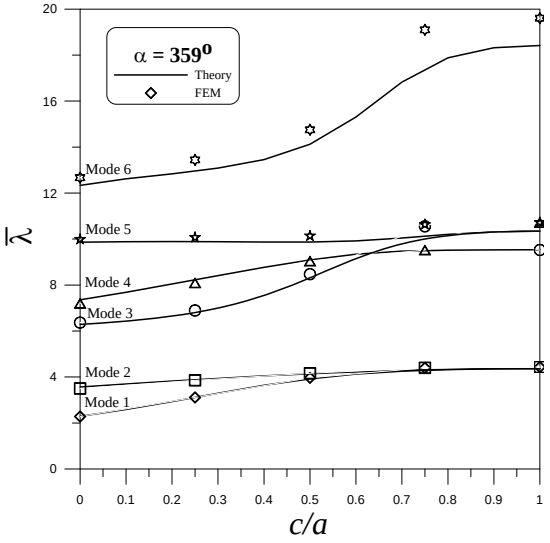


Fig. 8 The dependence of frequency parameter ($\bar{\lambda}$) versus notch depth ratios (c/a) for the V-notching piezoceramic plate with α = 359°.

4. CONCLUSIONS

Many researches and applications have addressed the vibration analysis for complete piezoceramic circular plates, but there are relatively scarce results about the plates with faults. In this study, the Ritz's method together with equivalent constants provides a more convenient strategy to investigate the transverse vibration characteristics of completely free piezoceramic circular plates with V-notches. The advantage of using the proposed methodology is that the electrical field consideration can be neglected, and so the vibration analysis of piezoceramic plates is carried out once the corresponding conditions of isotropic plates are given. Because the corresponding cases for isotropic plates are usually available in the literature, the transverse vibration analysis for piezoceramic plates can be simplified in this manner. To verify the theoretical predictions, numerical calculations are performed using the FEM; consistency between these two results implies that the theoretical approach has good accuracy for the transverse resonant frequencies. Through means of the defined non-dimensional frequency parameter, influence of the corner angle and depth of notch on the vibration behavior of V-notching circular plates is discussed in detail. As a response to the existence of V-notches, it is demonstrated that the order of mode shapes is not permanent and may exchange with each other. Moreover, both the mass and stiffness diminution of the piezoceramic circular plate with a V-notch typically affect the variation tendency of resonant frequencies, which depends on the values α = 180° or

https://doi.org/10.1017/jmech.2014.53 Published online by Cambridge University Press

359°. Following the theoretical analysis, the experimental measurement will be undertaken to validate the theoretical and numerical results in the subsequent work.

ACKNOWLEDGEMENTS

The authors gratefully acknowledge the financial support of this research by the National Science Council (Republic of China) under Grant NSC 94-2212-E-231-004.

REFERENCES

1. Tiersten, H. F., *Linear Piezoelectric Plate Vibrations*, Plenum Press, New York, U.S.A. (1969).
2. Holland, R., "Contour Extensional Resonant Properties of Rectangular Piezoelectric Plates," *IEEE Transactions on Sonics and Ultrasonics*, **15**, pp. 97–105 (1968).
3. Eer Nisse, E. P., "Variational Method for Electroelastic Vibration Analysis," *IEEE Transactions on Sonics and Ultrasonics*, **14**, pp. 153–160 (1967).
4. Shaw, E. A. G., "On the Resonant Vibrations of Thick Barium Titanate Disks," *Journal of the Acoustical Society of America*, **28**, pp. 38–50 (1956).
5. Kunkel, H. A., Locke, S. and Pikeroen, B., "Finite-element Analysis of Vibrational Modes in Piezoelectric Ceramics Disks," *IEEE Transactions on Ultrasonics, Ferroelectrics and Frequency Control*, **37**, pp. 316–328 (1990).
6. Guo, N., Cawley, P. and Hitchings, D., "The Finite Element Analysis of the Vibration Characteristics of Piezoelectric Discs," *Journal of Sound and Vibration*, **159**, pp. 115–138 (1992).
7. Ivina, N. F., "Numerical Analysis of the Normal Modes of Circular Piezoelectric Plates of Finite Dimensions," *Soviet Physics Acoustics*, **35**, pp. 385–388 (1990).
8. Huang, C. H., "Resonant Vibration Investigations for Piezoceramic Disks and Annuli by Using the Equivalent Constant Method," *IEEE Transactions on Ultrasonics, Ferroelectrics and Frequency Control*, **52**, pp. 1217–1228 (2005).
9. Huang, C. H. and Chen, Y. Y., "Transverse Vibration Analysis for Piezoceramic Rectangular Plates using Ritz's Method with Equivalent Constants," *IEEE Transactions on Ultrasonics, Ferroelectrics and Frequency Control*, **53**, pp. 265–273 (2006).
10. Leissa, A. W., McGee, O. G. and Huang, C. S., "Vibrations of Circular Plates Having V-Notches or Sharp Radial Cracks," *Journal of Sound and Vibration*, **161**, pp. 227–239 (1993).
11. McGee, O. G., Leissa, A. W., Huang, C. S. and Kim, J. W., "Vibrations of Circular plates with Clamped V-Notches or Rigidly Constrained Radial Cracks," *Journal of Sound and Vibration*, **181**, pp. 185–201 (1995).
12. McGee, O. G., Leissa, A. W., Kim, J. W. and Kim, Y. S., "Vibration of Plates with Constrained V-Notches or Cracks," *Journal of Engineering Mechanics*, **129**, pp. 812–822 (2003).
13. Williams, M. L., "Surface Stress Singularities resulting form Various Boundary Conditions in Angular Plates under Bending," *Proceeding of the First U.S. National Congress of Applied Mechanics*, U.S.A., pp. 325–329 (1952).
14. *ABAQUS User's Manual*, ver. 6.3, Pawtucket RI: Hibbit, Karlsson, and Sorensen, Inc., U.S.A. (2002).

(Manuscript received August 27, 2013,
accepted for publication March 17, 2014.)

https://doi.org/10.1017/jmech.2014.53 Published online by Cambridge University Press